# Tracking of Time-varying Mobile Radio Channels
# Part II: A Case Study

Lars Lindbom, Anders Ahlén, Mikael Sternad and Magnus Falkenström *

July 2, 2001

*Abstract-* **Low-complexity WLMS adaptation algorithms, of use for channel estimation, have been derived in a companion paper. They are here evaluated on the fast fading radio channels encountered in IS-136 TDMA systems, with the aim of clarifying several issues: How much can channel estimation performance be improved with these tools, as compared to LMS adaptation? When can an improved tracking MSE be expected to result in a meaningful reduction of the bit error rate? Will optimal prediction of future channel estimates significantly improve the equalization? Can one single tracker with fixed gain be used for all encountered Doppler frequencies and SNRs, or must a more elaborate scheme be adopted?**

**These questions are here investigated both analytically and by simulation. An exact analytical expression for the tracking MSE on two-tap FIR channels is presented and utilized. With this tool, the MSE performance and robustness of WLMS algorithms based on different statistical models can be investigated. A simulation study then compares the uncoded bit error rate of detectors, where channel trackers are used in decision directed mode in conjunction with Viterbi algorithms. A Viterbi detector combined with WLMS, based on second order autoregressive fading models possibly combined with integration, provides good performance and robustness at a reasonable complexity.**

*Keywords:* Adaptive estimation, fading channels, prediction methods, Least mean square methods.

## I. Introduction

In IS-136 digital mobile TDMA systems, a relatively low symbol rate and long data slots (6.67 ms) cause severe fading. In such 1900 MHz systems, one or two fading dips can be expected within each data slot. Furthermore, large variations in fading rates and frequency selectivity are encountered, so well designed channel estimators are crucial for obtaining adequate performance. Estimates obtained from training sequences (synchronization words) cannot be used within the whole slot and interpolation of channel estimates between training sequences [15] here provides inadequate performance. The same is true for decision-directed LMS and RLS adaptation. A Kalman filter with time-varying gain [3] would provide optimal performance, but it requires an on-line update of the adaptation gain in every sample. This solution has so far been deemed too complex.

The Wiener LMS (WLMS) algorithm, which has constant gain but can efficiently utilize the fading statistics, was presented in Part I of this paper [14]. It enables a systematic and structured design of high-performance adaptation laws with LMS computational complexity. An early design related to this class of algorithms [10] has been successfully applied to tracking problems in IS-136 TDMA systems [1, 8, 19].

We will here investigate the application of WLMS algorithms to the estimation of such fading channels. With large variations in the fading rate, a key issue is the selection of appropriate statistical fading models (*hypermodels*). Several design approaches can be conceived, some of which are listed below in decreasing order of complexity.

1. An autoregressive model for fading channel taps may be adjusted on line. This estimator can be implemented jointly with a WLMS algorithm or a Kalman tracker [25].

2. Some fading models, in particular Jakes' model [7], are specified by a few parameters, such as the speed of the mobile, which may be estimated separately. A set of WLMS algorithms can be pre-designed within a grid of these and other parameters. The parameters are estimated on line, and the appropriately tuned algorithm is selected. This *grid approach* [6] is sometimes called gain scheduling.

3. A single robustly designed algorithm might provide adequate performance over a wide range of Doppler shifts and disturbance levels.

At present, we consider alternative 1 to be far too complex, and possibly non-robust. The grid approach seems reasonable and has in [6] been found to work well. The use of a single fixed adaptive algorithm may at first sight seem over-optimistic, but it turns out to be feasible. The present paper will explore properties of the WLMS

*Lars Lindbom and Magnus Falkenström are with Ericsson Infotech, PO Box 1038, SE-65115 Karlstad, Sweden. Anders Ahlén and Mikael Sternad are with Signals and Systems, Uppsala University, PO Box 528, SE-75120, Uppsala, Sweden. Phone +46 4713076, fax +46 18 555096, aa@signal.uu.se, ms@signal.uu.se

algorithm which are relevant when using either a grid approach or a single robustly designed tracker.

The channel model will be outlined in Section II and in Section III, the WLMS algorithm is summarized. Section IV describes the choice of hypermodel structure. It then discusses the adjustment of autoregressive models to the fading statistics generated by isotropic scattering, for known as well as for uncertain Doppler frequencies.

Analytical expressions for the steady state mean square parameter tracking error are presented in Section V. In this case study, with a two-tap fading channel and a symbol alphabet with constant modulus, an *exact* performance analysis can be performed.

In Section VI, the tracking performance is investigated for fading rates at which the adaptation laws are tuned, as well as for other fading rates. The use of predicted channel estimates is also investigated and is shown to improve the performance significantly.

The bit error rate performance is finally evaluated by simulation in Section VII, for adaptive Viterbi detectors working in decision-directed mode. A peculiar nonlinear effect that appears when estimating flat fading channels is here discovered and discussed.

# II. The Channel Model

A sampled symbol-spaced baseband radio channel is described by the time-varying linear regression

$$y_t = (u_t \dots u_{t-M+1}) \begin{pmatrix} h_{0,t} \\ \vdots \\ h_{M-1,t} \end{pmatrix} + v_t = \varphi_t^* h_t + v_t \quad (1)$$

where $y_t$, here assumed to be a scalar[1], is the received signal at discrete time $t$. The complex-valued fading M-tap channel is represented by $h_t$. In IS-136 systems, it is reasonable to assume M=1 (flat fading) or M=2. The symbols $\{u_t\}$ are assumed to have zero mean and constant modulus. The regressor vector $\varphi_t^*$ is defined as the complex conjugate transpose of a column vector $\varphi_t$ that appears in the adaptation algorithms. It is assumed stationary with a known non-singular autocorrelation matrix $\mathbf{R} = \mathrm{E}\,\varphi_t \varphi_t^*$. The noise $v_t$ has zero mean and variance $\sigma_v^2$.

The fading properties of the channel coefficients will depend on the maximum Doppler frequency

$$\omega_{\mathrm{D}} = 2\pi f_{\mathrm{D}} = 2\pi v_o / \lambda \qquad \text{(rad/s)} \quad (2)$$

where $v_o$ denotes the speed of the mobile and $\lambda$ is the carrier wavelength, which in the following is assumed to be 16cm (~1900 MHz). For the purpose of our channel estimator design demonstrations, we mainly assume Jakes' fading model [7]. When $v_o$ is constant, the channel coefficients will then be stationary, circular Gaussian processes with zero means and covariance function

$$r_h(\ell) = \mathrm{E}\, h_t h_{t-\ell}^* = \mathbf{R}_h J_0(\Omega_{\mathrm{D}}\, \ell) \qquad \ell = 0, \pm 1, \cdots \quad (3)$$

which yields the classical fading spectrum

$$\phi_h(\Omega) = \begin{cases} \frac{2}{\sqrt{\Omega_D^2 - \Omega^2}} \mathbf{R}_h & |\Omega| < \Omega_{\mathrm{D}} \\ 0 & |\Omega| > \Omega_{\mathrm{D}} \end{cases} . \quad (4)$$

Here, $\mathbf{R}_h = \mathrm{E}\, h_t h_t^*$, while $J_0(\cdot)$ denotes the Bessel function of the first kind and zero order and

$$\Omega = \omega T \quad ; \quad \Omega_{\mathrm{D}} = \omega_{\mathrm{D}} T \quad . \quad (5)$$

The symbol time $T$ will be set to 41.15$\mu$s as in IS-136.

# III. The Channel Estimator

We shall use the WLMS-algorithm presented in Part I of this paper [14] to track and predict the channel $h_t$. To describe $h_t$, we shall use simplified fading models in the form of marginally stable autoregressive models of order $n_D$, with equal dynamics for all channel taps

$$\bar{h}_t = \frac{1}{D(q^{-1})} \mathbf{I}\, e_t = \frac{1}{1 + d_1 q^{-1} + \ldots + d_{n_D} q^{-n_D}} \mathbf{I}\, e_t \quad . \quad (6)$$

The notation $\bar{h}_t$ is introduced to indicate that (6) will not be a perfect description of $h_t$. Here, $q^{-1}$ denotes the backward shift operator ($q^{-1} y_t = y_{t-1}$) and $e_t$ is a white zero mean random vector sequence with covariance matrix $\mathbf{R}_e$. For symmetric fading spectra, the scalar coefficients $\{d_i\}$ can be assumed real-valued.

The model (6) should approximate the essential behavior of the time variability, in our case described by the autocorrelation function (3). When (6), $\mathbf{R}_e, \mathbf{R}$ and $\sigma_v$ are given, Theorem 1 of [14] directly provides an optimized WLMS-algorithm for tracking the parameter vector $h_t$ in (1):

$$\begin{aligned} \varepsilon_t &= y_t - \varphi_t^* \hat{h}_{t|t-1} && (7) \\ \hat{h}_t &= \hat{h}_{t|t-1} + \mu \mathbf{R}^{-1} \varphi_t \varepsilon_t && (8) \\ \hat{h}_{t+k|t} &= \frac{Q_k(q^{-1})}{Q_0(q^{-1})} \mathbf{I}\, \hat{h}_t \quad . && (9) \end{aligned}$$

Here, $\hat{h}_{t+k|t}$ denotes an estimate of $h_{t+k}$ at discrete time $t$ and $\hat{h}_t = \hat{h}_{t|t}$. The scalar gain $\mu$ is a step size parameter, and (9) is the coefficient smoothing-prediction estimator. An alternative equivalent implementation can be expressed in terms of the *learning filter* $\boldsymbol{\mathcal{L}}_k(q^{-1})$ [14]:

$$\begin{aligned} f_t &= \mathbf{R} \hat{h}_{t|t-1} + \varphi_t \varepsilon_t \\ \hat{h}_{t+k|t} &= \boldsymbol{\mathcal{L}}_k(q^{-1}) f_t = \frac{Q_k(q^{-1})}{\beta(q^{-1})} \mathbf{R}^{-1} f_t \quad . \quad (10) \end{aligned}$$

[1] The tracking and equalization algorithms are applicable also to vector signals, which appear in multiple antenna systems and when sampling faster than the symbol rate. See [12] for a design example.

where

$$\beta(q^{-1}) = D(q^{-1}) + q^{-1}Q_1(q^{-1}) \quad .$$

The polynomials $Q_i(q^{-1})$ depend on the selected hypermodel (6) and are calculated via Theorem 1 in [14] to minimize the mean square parameter error

$$\mathrm{E}\,|\tilde{h}_{t+k|t}|^2 \;=\; \mathrm{tr}\,\mathrm{E}\,\tilde{h}_{t+k|t}\tilde{h}^*_{t+k|t} \stackrel{\Delta}{=} \;\mathrm{tr}\,\mathbf{P}_k \qquad (11)$$

where

$$\tilde{h}_{t+k|t} = h_{t+k} - \hat{h}_{t+k|t} \quad .$$

# IV. Dynamic fading models

## A. Autoregressive/integrating models

An exact representation of the fading statistics (3)-(4) would require the use of an autoregressive fading model (6) of infinite order. We will here use and compare the following special cases of (6).

1. **RW**, Random walk modelling, $D(q^{-1}) = 1 - q^{-1}$, results in an LMS algorithm. It is a common first choice when no prior information is available [2].

2. **FRW** (Filtered random walk):

   $$D(q^{-1}) = (1 - q^{-1})(1 - aq^{-1}) \quad ,$$

   with $|a| \le 1$, is a useful model in many situations. The special case of an integrated random walk (**IRW**, $a = 1$), will be appropriate if the short term behavior is well approximated by linear trends.

3. $\mathbf{AR}_2$ (Autoregressive second order model):

   $$D(q^{-1}) = 1 - 2\rho\cos\omega_o q^{-1} + \rho^2 q^{-2} \quad .$$

   Here, $\rho$ and $\omega_o$ determine the degree of damping and the dominating frequency, respectively. For Jakes fading models (3), a reasonable bandwidth is obtained with $\omega_o = \Omega^o_{\mathrm{D}}/\sqrt{2}$ where $\Omega^o_{\mathrm{D}}$ is a nominal or estimated Doppler frequency.

4. $\mathbf{AR}_2\mathbf{I}$ (Autoregressive and integrating model):

   $$D(q^{-1}) = (1 - 2\rho\cos\frac{\Omega^o_{\mathrm{D}}}{\sqrt{2}}q^{-1} + \rho^2 q^{-2})(1 - q^{-1}) \quad .$$

   This model is useful when some parameters are oscillating while others are slowly varying or constant. The integrating term $(1 - q^{-1})$ will guarantee an unbiased estimate of constant parameters when $\mathbf{R}$ is nonsingular, see (42) in [14]. The $\mathrm{AR}_2\mathrm{I}$ model is also of use for long-range prediction of oscillations around a nonzero mean, which occurs in Rician fading; without an integrating model factor, prediction estimates would in that case be biased towards zero.

5. $\mathbf{AR}_{n_D}$, autoregressive models of order $n_D = 3$ or higher, are appropriate when important properties of the covariance function of the time-variation are difficult to match with a few parameters. Their adjustment is described in Section IV.B below.

Design based on RW modelling results in an LMS algorithm, while FRW or $\mathrm{AR}_2$ modelling leads to a simplified Wiener LMS algorithm, which is simple to design and to readjust on-line, see Section IV of [14]. With $\mathrm{AR}_2\mathrm{I}$ or $\mathrm{AR}_{n_D}$ models, readjustment of the algorithm (at most once per slot) will require the numerical solution of a polynomial spectral factorization of order $n_D$.

When using $\mathrm{AR}_2$ and $\mathrm{AR}_2\mathrm{I}$ models, we need to select the parameters $\Omega^o_{\mathrm{D}}$ and $\rho$. In this case study, the pole radius $\rho$ is fairly easy to select. For maximum normalized Doppler frequencies of interest here, $\Omega_{\mathrm{D}} < 0.1$, the value $\rho = 0.999 - 0.1\Omega_{\mathrm{D}}$ is by our experience reasonable for Jakes' model. Then, $\Omega^o_{\mathrm{D}}$ is set to $\Omega_{\mathrm{D}}$ which can be estimated on line reasonably well using either the assumed correlation Bessel function (3) of the fading pattern [11], or level crossing rates.

## B. Adjusting AR Model Parameters to Fading Covariance Statistics

The adjustment of (6)

$$\bar{h}_t + d_1\bar{h}_{t-1} + \ldots + d_{n_D}\bar{h}_{t-n_D} = e_t \qquad (12)$$

can be based directly on a known or estimated covariance function. We can adjust $D(q^{-1})$ by considering row $j$ of (12). Introduce the set of covariances

$$\{\bar{r}_{\ell_i} \stackrel{\Delta}{=} \mathrm{E}\,\bar{h}_{j,t}\bar{h}^*_{j,t-\ell_i}\}_{i=1}^N \quad ,$$

where $\bar{h}_{j,t}$ denotes element (tap) $j$ of $\bar{h}_t$ and where $\ell_i$ are integers such that $0 < \ell_1 < \ldots < \ell_N$. Multiplying row $j$ of (12) by $\bar{h}^*_{j,t-\ell_i}$ and taking the expectation gives the equations

$$\bar{r}_{\ell_i} + d_1\bar{r}_{\ell_i-1} + \ldots + d_{n_D}\bar{r}_{\ell_i-n_D} = 0 \qquad i = 1, 2, \ldots, N \,. \qquad (13)$$

In the particular case of $\ell_i = i$ and $N = n_D$, we obtain the Yule-Walker equations. However, $N$ might very well be chosen much larger than $n_D$ and the time-lags $\ell_i$ can be distributed over a large interval.

The covariances $\bar{r}_j$ can be replaced by data-based estimates. The resulting polynomial $D(z^{-1})$ could then have roots outside the unit circle, and should in that case be adjusted so that all roots are in $|z| \le 1$. Estimation of $\bar{r}_j$ based on data, as suggested in [25], will require an initial training period of considerable length and will give reliable estimates only at high SNR's.

We therefore prefer to use theoretical expressions for the covariances, parametrized by the maximum Doppler frequency. When adjusting the AR model to the fading model (3), we replace $\bar{r}_{\ell_i-w}$ in (13) by $J_0(\Omega_{\mathrm{D}}(\ell_i - w))$ and solve the possibly over-determined system of equations by the least squares method.

[2]However, in such cases we would rather advocate the use of filtered random walk modelling with $a \in [0.9 - 0.999]$.

In Figure 1, the Bessel function in (3) for $\Omega_{\mathrm{D}} = 0.02$ (45 km/h) is compared to the $\mathrm{AR}_3$ covariance function adjusted with $N = 6$, for $\ell_N = 61$ and $\ell_N = 251$. Clearly, including higher-lag covariances in (13) yields a better agreement between the Bessel function and the AR model for large lags.

The correlation between taps, modelled by $\mathbf{R}_h$ in (3) and $\mathbf{R}_e$ in (6), can be estimated from data. With well synchronized IS-136 receivers, the tap correlation will be small.

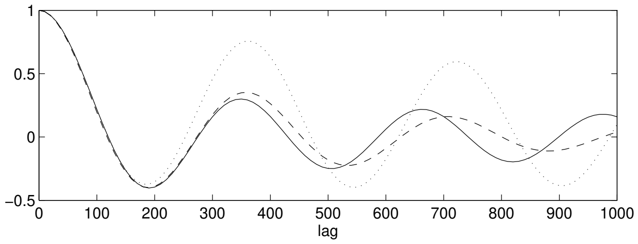


Figure 1: Adjusting third order AR hypermodels to the Bessel function $J_0(\Omega_{\mathrm{D}}\ell)$, at $\Omega_{\mathrm{D}} = 0.02$ (45km/h), (solid) according to (13) at six evenly spaced points, for the maximum lag $\ell_N = 61$ (dotted) and $\ell_N = 251$ (dashed).

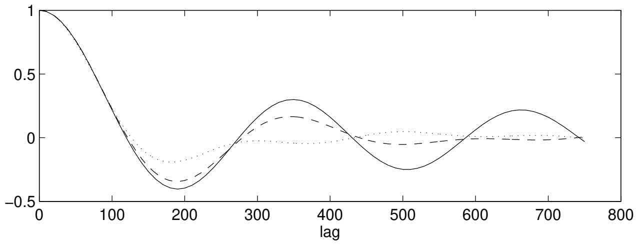


Figure 2: Auto-covariance function $r_h(\ell) = J_0(\Omega_{\mathrm{D}}\ell)$ with $\Omega_{\mathrm{D}} = 0.02$ (solid) and the averaged covariance function (15), with $\Omega_{\mathrm{D}} \in U[0.01\ \ 0.03]$ (dotted) and $\Omega_{\mathrm{D}} \in U[0.015\ \ 0.025]$ (dashed).

## C. Robust Design of Adaptation Laws

If the Doppler frequency $\Omega_{\mathrm{D}}$ is uncertain, one could minimize the worst-case effect of this uncertainty by performing a minimax robust filter design [9, 18]. A less conservative, and often much less computationally demanding, alternative is to regard $\Omega_{\mathrm{D}}$ as a random variable. The MSE tracking performance resulting from the outcomes of $\Omega_{\mathrm{D}}$ is averaged and we minimize this average [23, 26]. As is shown in [24] and Section 3.5 of [11], this problem can be solved by spectrally *averaging over the hypermodels* (6). Such averaging has also been used in Section IV.A of [17]. A Doppler spectrum averaged with respect to an uncertain parameter $\Omega_{\mathrm{D}}$ is given by

$$\tilde{\phi_h}(\Omega) \triangleq \mathrm{E}\,\phi_h(\Omega) = \int_{-\pi}^{\pi} \phi_h(\Omega, \Omega_{\mathrm{D}}) p(\Omega_{\mathrm{D}})\, d\Omega_{\mathrm{D}} \qquad (14)$$

where $\phi_h(\Omega, \Omega_{\mathrm{D}})$ represents the spectrum of the channel coefficients and $p(\Omega_{\mathrm{D}})$ denotes the probability density function of the normalized maximum Doppler frequency $\Omega_{\mathrm{D}}$. When assuming Jakes model and (3), the covariance function corresponding to (14) is

$$\tilde{r}_h(\ell) \triangleq \int_{-\pi}^{\pi} r_h(\ell)\, p(\Omega_{\mathrm{D}})\, d\Omega_{\mathrm{D}} = \int_{-\pi}^{\pi} \mathbf{R}_h J_0(\Omega_{\mathrm{D}}\,\ell) p(\Omega_{\mathrm{D}})\, d\Omega_{\mathrm{D}} \qquad (15)$$

An averaged AR hypermodel can now be adjusted using $\tilde{r}_h(\ell)$ instead of $\bar{r}_h(\ell)$. A robust tracking algorithm can then be designed using this model.

In Figure 2, the averaged covariance function (15) is displayed for a uniformly distributed probability density function $p(\Omega_{\mathrm{D}})$ with different uncertainty regions. A wider uncertainty region will increase the damping of the averaged covariance function, yielding a spectrum with a less pronounced peak.

Deviations from Jakes' model can be regarded as unstructured uncertainty, which can be incorporated in an averaged robust design, see [11, 26, 23].

# V. Performance Analysis

Based on *two-tap* channel models (1) and on a known fading model such as Jakes' model (3), we can obtain an exact expression for the steady state tracking MSE, $\mathrm{tr}\,\mathbf{P}_k$. The expression is valid for arbitrarily fast fading and for all algorithms with WLMS structure. Introduce the learning filter gain

$$\Sigma_k = \frac{1}{2\pi}\int_{-\pi}^{\pi} \left| \frac{Q_k(e^{\jmath\Omega})}{\beta(e^{\jmath\Omega})} \right|^2 d\Omega \ . \qquad (16)$$

*Lemma 1.* Consider the channel model (1), with $M < 3$. Assume $h_t$, $\varphi_t^*$ and $v_t$ to be mutually independent and stationary. Let the fading channel coefficient vector have spectrum $\phi_h(\Omega)$ and covariance matrix $\mathrm{E}\,h_t h_t^* = \mathbf{R}_h$. The zero mean noise $v_t$ has variance $\sigma_v^2$. Let the zero mean symbols $u_t$ be uncorrelated in time, with constant modulus and variance $\sigma_u^2$ ($\mathbf{R} = \sigma_u^2\mathbf{I}$). Assume $(M-1)\Sigma_1 < 1$. If an estimator for $h_{t+k}$ with the structure (10) or (7)–(9) is used, then the steady-state mean square estimation error (11) is given by

$$\mathrm{tr}\,\mathbf{P}_k = \frac{\Gamma_k + \mathrm{M}\,10^{-\frac{\mathrm{SNR}}{10}}\,\Sigma_k + (\mathrm{M}-1)G_k}{1-(\mathrm{M}-1)\Sigma_1}\,\mathrm{tr}\,\mathbf{R}_h \qquad (17)$$

where

$$\Gamma_k = \frac{1}{2\pi}\int_{-\pi}^{\pi} \left| \frac{\beta(e^{\jmath\Omega}) - e^{\jmath\Omega k}Q_k(e^{\jmath\Omega})}{\beta(e^{\jmath\Omega})} \right|^2 \frac{\mathrm{tr}\,\phi_h}{\mathrm{tr}\,\mathbf{R}_h}\, d\Omega \qquad (18)$$

$$G_k = \Gamma_1\Sigma_k - \Gamma_k\Sigma_1 \qquad (19)$$

and

$$\mathrm{SNR} \triangleq 10\log\frac{\sigma_u^2}{\sigma_v^2}\mathrm{E}\,|h_t|^2 \qquad (\mathrm{dB}) \qquad (20)$$

□

Proof: Obtained from [13] for constant modulus regressors (with kurtosis 1), by observing that $\mathrm{tr}\,\mathbf{V}_h^k =$

$\mathrm{tr}\,\mathbf{R}_h\Gamma_k$ and $\mathrm{E}\,|h_t|^2 = \mathrm{tr}\,\mathbf{R}_h$.

Lemma 1 holds exactly for $M < 3$, but is a good approximation also for higher order FIR channels.

Above, $(M-1)\Sigma_1 < 1$ is a condition for convergence in MSE. This condition will always be fulfilled for flat fading channels. Note also that the term $G_k$ vanishes for $k = 1$. All preconditions for Lemma 1 are fulfilled in the IS-136 TDMA system: The symbols $u_t$ are uncorrelated due to the interleaving and are circular with constant modulus. The delay spread is not larger than one symbol interval $T$, so channel models with $M \leq 2$ are appropriate. The term $v_t$ represents mainly co-channel interference and thermal noise. It can be assumed zero mean and independent of both $u_\tau$ and $h_\tau$ for all $\tau$.

For filters and smoothers (7)-(9) designed to minimize (11) based on perfect models, the error will vanish with a vanishing noise variance.

For predictors, the tracking error (17) will not vanish even in the noise-free case, and it will increase with the fading rate. It decreases if more accurate AR-approximations of the true fading spectrum $\phi_h$ are used in the WLMS design.

It is of interest to know to what extent improved linear regression modelling of the parameter dynamics can improve the end result for which it is intended. Filtering or detection performance is essentially determined by the ambient SNR. With Lemma 1, the variance of the "tracking noise" $\sum_{i=0}^{M-1} \tilde{h}_{i,t|t-k} u_{t-i}$, caused by non-perfect tracking, can be calculated and compared to the variance of the noise $v_t$. As a rough but useful performance indicator, we define the relative noise level

$$V \triangleq 10 \log \left( \frac{\sigma_u^2 \mathrm{tr}\,\mathbf{P}_k + \sigma_v^2}{\sigma_v^2} \right) \quad \text{(dB)} \qquad (21)$$

where the numerator describes the variance in $y_t - \varphi_t^* \hat{h}_{t|t-k}$ due to the tracking error plus noise, if $\tilde{h}, u$ and $v$ are mutually uncorrelated. We can use the increase of the noise level to predict the performance deterioration in e.g. an equalizer[3].

When $V$ is above 3dB, the tracking noise dominates over the output noise $v_t$. It is then worthwhile to consider a superior adaptation law based on, for example, a higher order hypermodel. If $V$ is below 1dB, then the noise $v_t$ dominates, so even a total elimination of the tracking errors would result in marginal improvements of the performance of a filter or detector based on the estimated model.

# VI. MSE Performance

We will here investigate the performance of the tracking algorithm theoretically, by using Lemma 1 for two-tap Rayleigh fading channels with taps of equal variance, and regressors with constant modulus and variance 1.

[3]A similar investigation is performed for Kalman trackers and decision feedback equalizers in [22].

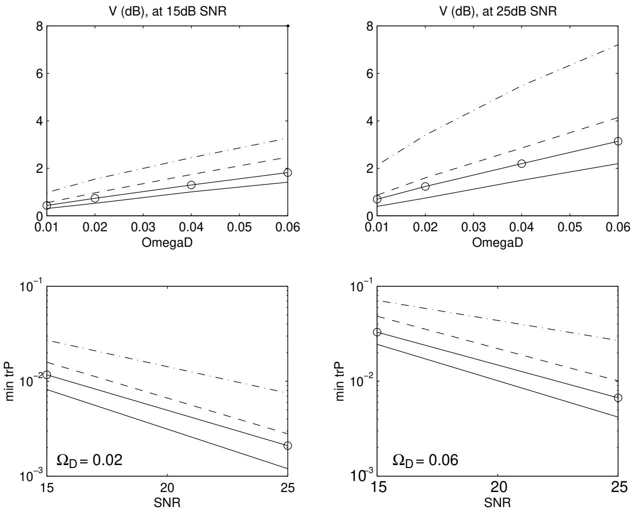


Figure 3: Optimized tracking error $\mathrm{E}\,\|\tilde{h}_{t+1|t}\|_2^2 = \mathrm{tr}\,\mathbf{P}_1$ (lower part) and relative tracking noise level $V$ (dB) (upper part) in Section VI for WLMS algorithms based on RW modelling (dashed-dotted), IRW (dashed) $\mathrm{AR}_2$ (circles) and $\mathrm{AR}_4$ (solid). All AR models are matched to the true normalized Doppler frequency $\Omega_{\mathrm{D}}$.

## A. MSE Performance: The Ideal Case

In the lower half of Figure 3, the mean square sum of tap prediction errors $\mathrm{tr}\,\mathbf{P}_1$ has been calculated by Lemma 1, using $\phi_h$ from (4) and $\mathrm{tr}\,\mathbf{R}_h = 2$. We investigate WLMS algorithms based on adjusted hypermodels of various structures, with optimized gains $\mu$, for SNR 15 dB to 25 dB. The corresponding numerical results are presented in Table 1. While the attainable performance improves with the complexity of the hypermodel, the use of increasingly complex models gives diminishing returns.

The top diagrams in Figure 3 display the relative tracking noise level (21), under the assumption $\sigma_u^2 = 1, \mathrm{E}\,|h_t^o|^2 = \mathrm{E}\,|h_t^1|^2 = 1$ and $\mathrm{SNR} = 10\log(2/\sigma_v^2)$. For LMS tracking (WLMS based on random walks), the tracking error is in many of the considered cases so large that it dominates over $v_t$ ($V > 3$dB in the upper diagrams of Figure 3). The tracking performance can be improved significantly by simply extending LMS (RW hypermodelling) with an integrator, i.e. by using an IRW hypermodel. If we use an $\mathrm{AR}_4$ model, we obtain a better tracking MSE for $\Omega_{\mathrm{D}} = 0.06$ ($\sim 140$ km/h) than can be obtained by using the RW model with $\Omega_{\mathrm{D}} = 0.02$ ($\sim 45$ km/h). In terms of the effect of the noise level on the tracking MSE, more than 10 dB can be gained at both $\Omega_{\mathrm{D}} = 0.02$ and $\Omega_{\mathrm{D}} = 0.06$ by using an $\mathrm{AR}_4$ model instead of a random walk model (bottom diagrams).

The properties of different adaptation algorithms can also be understood by comparing their learning filters (10). See Figure 4, which compares RW (LMS), $\mathrm{AR}_2$ and $\mathrm{AR}_2$I designs at $\Omega_{\mathrm{D}} = 0.04$.[4] The bandwidth of

[4]The tuned second order AR denominator is given by $D(q^{-1}) = 1 - 1.9891q^{-1} + 0.99003q^{-2}$. For 25dB, the tuned

Table 1: The attainable tracking error $\mathrm{tr}\,\mathbf{P}_1$ obtained by Lemma 1 for WLMS algorithms based on different hypermodels matched to the true Doppler frequency. For FRW, $a = 0.98$. Compare to Figure 3.

| $\Omega_D$ | 0.01 | | 0.02 | | 0.04 | | 0.06 | |
|---|---|---|---|---|---|---|---|---|
| SNR | 15 dB | 25 dB | 15 dB | 25 dB | 15 dB | 25 dB | 15 dB | 25 dB |
| RW | 0.0159 | 0.0040 | 0.0271 | 0.0075 | 0.0485 | 0.0160 | 0.0711 | 0.0269 |
| FRW | 0.0101 | 0.0019 | 0.0161 | 0.0030 | 0.0292 | 0.0058 | 0.0447 | 0.0096 |
| IRW | 0.0086 | 0.0014 | 0.0159 | 0.0028 | 0.0312 | 0.0059 | 0.0484 | 0.0101 |
| $AR_2$ | 0.0067 | 0.0011 | 0.0117 | 0.0021 | 0.0218 | 0.0042 | 0.0329 | 0.0067 |
| $AR_2I$ | 0.0057 | 0.0009 | 0.0108 | 0.0016 | 0.0203 | 0.0034 | 0.0329 | 0.0055 |
| $AR_3$ | 0.0050 | 0.0008 | 0.0092 | 0.0014 | 0.0175 | 0.0030 | 0.0264 | 0.0048 |
| $AR_4$ | 0.0047 | 0.0006 | 0.0082 | 0.0012 | 0.0165 | 0.0026 | 0.0245 | 0.0042 |

Table 2: As in Table 1 but for hypermodels matched to the fading statistics for an incorrect Doppler frequency. The minimal values of each column are emphasized.

| | $AR_{n_D}$ matched to $\Omega_D$ =0.02 | | | | $AR_{n_D}$ matched to $\Omega_D$ =0.04 | | | |
|---|---|---|---|---|---|---|---|---|
| $\Omega_D$ | 0.01 | | 0.04 | | 0.01 | | 0.02 | |
| SNR | 15 dB | 25 dB | 15 dB | 25 dB | 15 dB | 25 dB | 15 dB | 25 dB |
| $AR_2$ | 0.0122 | 0.0021 | 0.0279 | 0.0053 | 0.0257 | 0.0049 | 0.0231 | 0.0044 |
| $AR_2I$ | **0.0085** | **0.0013** | 0.0287 | 0.0045 | **0.0129** | **0.0022** | **0.0154** | **0.0025** |
| $AR_3$ | 0.0100 | 0.0015 | **0.0260** | **0.0042** | 0.0193 | 0.0033 | 0.0199 | 0.0034 |
| $AR_4$ | **0.0085** | **0.0013** | 0.0285 | **0.0042** | 0.0185 | 0.0029 | 0.0182 | 0.0029 |

the learning filter approaches $\Omega_D = 0.04$ as the SNR decreases but, as can be seen in Figure 4, it is significantly higher for moderate and high SNR's. The reason is that the lag error will, to a large extent, be determined by the phase lag introduced by the learning filter in frequency regions where $h_t$ has significant energy. When the noise level is low, a Wiener design can give priority to suppressing lag errors by attaining low phase shifts at these frequencies (at or below $\Omega_D = 0.04$), at the price of widening the bandwidth of the learning filter. When the SNR decreases, noise rejection is given higher priority.

Note that the RW/LMS learning filter has the highest gain at high frequencies. This makes this estimator most sensitive to noise.

## B. Mismatched Designs

The performance of incorrectly tuned algorithms has also been computed from Lemma 1 and are presented in Table 2. From Table 1 and Table 2, we can draw the following conclusions:

- If the Doppler frequency $\Omega_D$ is uncertain, $AR_2I$ modelling seems to be the best choice when $\Omega_D$ is overestimated. When $\Omega_D$ is underestimated, $AR_3$ models appear to perform slightly better. (Bold numbers in Table 2.)
- The use of a higher order AR hypermodel results in considerably better tracking performance than the use of a RW model, even if $\Omega_D^o$ is severely mismatched in the latter case (Table 1, Table 2).

In Figure 5, the tracking algorithms were matched to a maximum Doppler frequency of 140Hz ($\Omega_D = 0.035$) and an SNR of 15 dB. These results indicate that the $AR_2I$ hypermodel is a superior choice if we *underestimate* the SNR and *overestimate* the Doppler frequency.

The bottom line of the evaluation so far can be formulated as follows: *If an uncertain estimate of $\Omega_D$ is available, and low computational complexity is required, then use a WLMS algorithm based on a nominal $AR_2I$ hypermodel.* Select the design value $\Omega_D^0$ at the high end of the uncertainty interval of $\Omega_D$ and the design value of the SNR at the lower limit of its uncertainty range. Such a design should provide good performance for all Doppler frequencies from zero up to $\Omega_D^0$.

The robust averaged design proposed in Section IV.C has been investigated on IS-136 channels in [24], based on averaged $AR_3$ hypermodels. It turned out to give a further reduction of the averaged tracking MSE, as compared to designing for the maximal $\Omega_D^0$.

step length parameters $\mu$ are 0.36, 0.21 and 0.17 for RW, $AR_2$ and $AR_2I$-based designs, respectively. For 15dB, $\mu = 0.27, 0.13$ and 0.127, respectively.

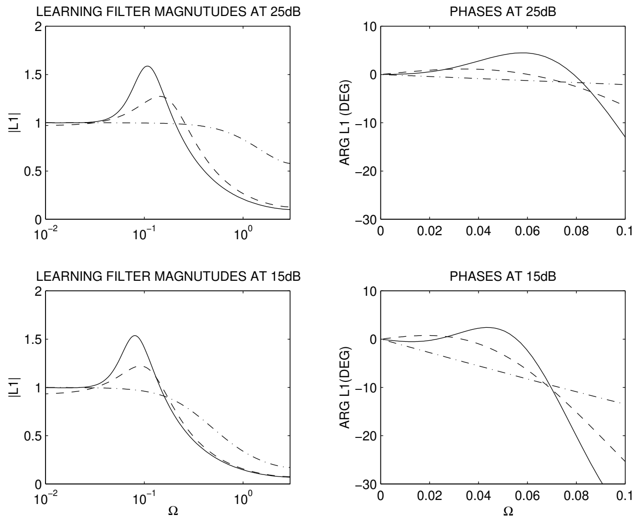


Figure 4: Learning filter magnitudes $|Q_1(e^{i\Omega})/\beta(e^{i\Omega})|$ (left) and phases (right) for optimally tuned WLMS algorithms based on RW (dash-dotted) $AR_2$ (dashed) and $AR_2I$ (solid) fading models at $\Omega_D = 0.04$ ($f_D = 160$Hz), for SNR=25dB and SNR=15dB, respectively.

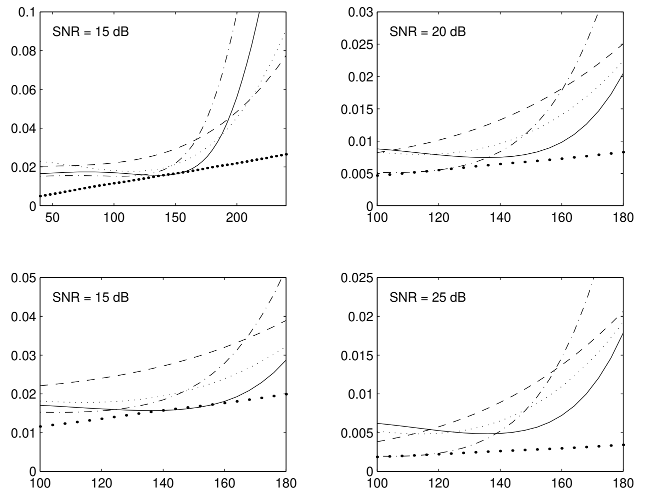


Figure 5: MSE performance $\mathrm{tr}\,\mathbf{P}_1$ as a function of $f_D$ for different choices of WLMS algorithms *matched to 140 Hz and 15 dB.* The algorithms are based on IRW (dashed), $AR_2$ (dotted), $AR_2I$ (dash-dotted) and $AR_3$ (solid) hypermodels. Compare to a fully matched $AR_3$ design (bulleted). The lower left-hand plot expands the upper left-hand diagram.

## C. Optimal Channel Prediction

Optimized channel predictors can be designed using either Kalman trackers or WLMS algorithms[5]. Figure 6 illustrates the MSE performance obtained by using $AR_3$ prediction (circles) instead of just extrapolating the current estimate into the future (crosses). The improvement is large and it increases with the prediction length. Naturally, the gain will increase with an increasing vehicle speed and a decreasing noise level. Similar, but somewhat smaller improvements were obtained when using $AR_2I$ and $AR_2$ hypermodels.

The use of this type of linear prediction can also be of interest e.g. for fast power control in CDMA systems. Long-range prediction is of interest for resource scheduling and adaptive modulation [4],[5].

# VII. Simulation Study

We shall investigate the bit error rate performance of adaptive decision-directed Viterbi receivers, as described by Figure 7. The channel estimator utilizes estimated symbols as regressors in decision-directed mode. It provides predicted channel taps, which are used in the metric computation of the Viterbi algorithm.

For adaptive detectors working in decision directed mode, the tracking is required to be accurate and robust against erroneous regressors, which will occur in particular around fading dips, where $|h_t|$ is small.

[5] The use of e.g an LMS filter estimate and a separate predictor for this time series [2] is a suboptimal alternative.

## A. Specifications

We focus on a set-up suitable for the IS-136 standard [20], with the following conditions.

- *Slot structure:* As in the forward link of IS-136 with $N = 162$ differential QPSK-modulated symbols, including $N_{tr} = 14$ leading training symbols.[6]
- *Channel properties:* A two tap Rayleigh fading symbol-spaced baseband channel model with independently fading taps[7] is simulated:

$$y_t = h_{0,t}u_t + h_{1,t}u_{t-1} + v_t \quad ; \quad \mathbf{R} = \mathbf{I} \qquad (22)$$

with $\mathbf{R}_e$ diagonal and $\mathrm{E}\,|h_{0,t}|^2 = \mathrm{E}\,|h_{1,t}|^2 = 1$. The taps $h_{i,t}$ are generated according to [7], using 12 offset oscillators with uniformly distributed ($[0, 2\pi]$) phases. Hence, the level crossing statistics is close to that of a classical Rayleigh fading environment. All estimators are initialized from least squares estimates of the channel taps in the form of robustified linear trends, based on the initial training sequence[8]. We also study the flat fading case.

[6] A known CDVCC sequence of six differential symbols is placed after 85 symbols of the slot. It is here not used to improve the tracking performance, since this would complicate the performance evaluation.

[7] The more realistic case of correlated taps would result in higher bit error rates due to partial loss of diversity, but will otherwise not provide any new fundamental problems for the tracking.

[8] Since the slope of a linear trend will be more uncertain than its average level, we initialize the model as

$$\hat{y}_t = (h_{0,\ell}+(t-8)\alpha h_{0,s})u(t)+(h_{1,\ell}+(t-8)\alpha h_{1,s})u(t-1)\ ;\ t = 2\dots 15$$

where $\alpha = \mathrm{SIR}/22$ for $0 < \mathrm{SIR} < 22$dB, with SIR being the signal-to-interference ratio estimated from the model residuals during the training phase. Here, $h_{i,\ell}$ and $h_{i,s}$ are estimated

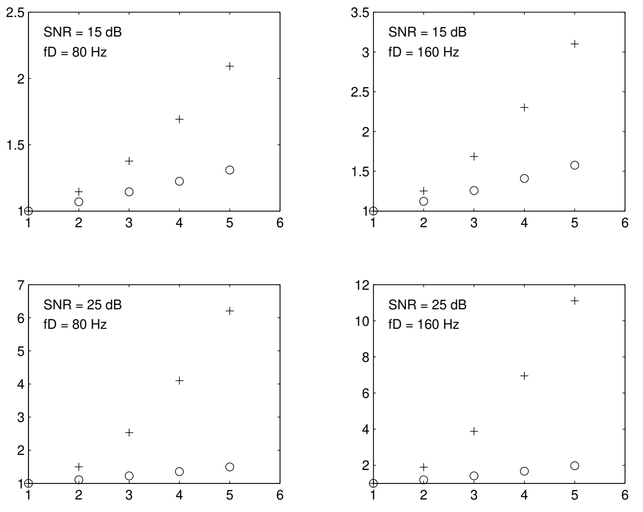


Figure 6: Relative MSE increase $\mathrm{tr}\,\mathbf{P}_k/\mathrm{tr}\,\mathbf{P}_1$, of $k-$step channel prediction of Rayleigh fading channel taps, compared to one-step prediction, as a function of $k$. The most recent channel estimate used as $k$-step predictor (crosses) is compared to the use of an optimal $k$-step predictor (circles), for $AR_3$-based WLMS tracking algorithms.

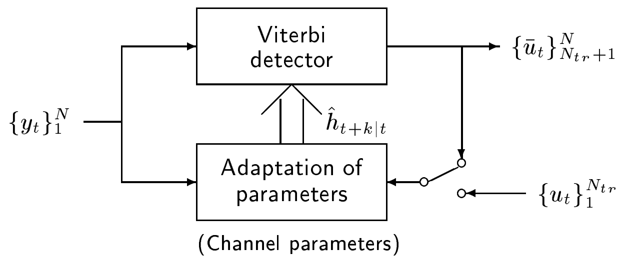


Figure 7: Adaptive equalization based on decision directed channel estimation. In learning-directed mode, the adaptation is based on training data. At time instant $t = N_{tr} + 1$, the adaptation is switched into decision-directed mode and decisioned symbols $\bar{u}_t$ are used as regressor variables.

- *Disturbance properties:* The scenario is interference-limited with burst-synchronized interferers propagating via the same type of fading channel as the signal. In the simulations, the interference was also symbol-synchronized. The color of the interference is not estimated. (In a noise-limited scenario with Gaussian noise, the BER performance improves.)

- *Idealized simulation conditions:* To isolate the tracking properties, we have compared decision directed adaptation to the use of correct symbols $u_t$ as regressors. To quantify the loss of performance due to imperfect initialization, we also compare to initialization with known channel taps.

jointly by off-line least squares. The robustification parameter $\alpha$ de-emphasizes uncertain slope estimates at low SIRs.

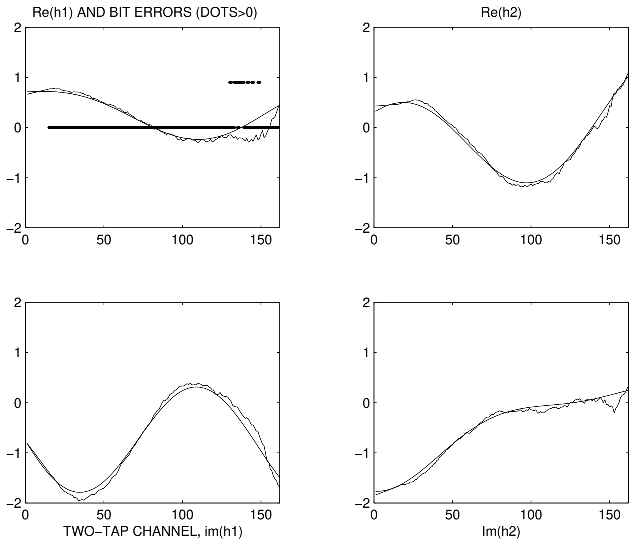


Figure 8: Real and imaginary parts of tap 1 and tap 2, showing true trajectories and estimates by an $AR_2$I-designed WLMS algorithm at SIR=20dB. In the upper left figure, dots at the zero level symbolize correct decisions while dots at level 0.9 indicate decision errors.

## B. BER Performance at 90km/h

WLMS tracking algorithms based on random walk (LMS), $AR_2$ and $AR_2$I fading models are now evaluated in combination with a Viterbi algorithm at $\Omega_D = 0.04$, or $f_D = 160$Hz (speed 90km/h).

Table 3: Adaptive equalization of the channel (22) at $\Omega_D = 0.04$ with $\mathrm{E}\,|h_{0,t}|^2 = \mathrm{E}\,|h_{1,t}|^2 = 1$. 10000 slots per simulation case. In the lower part of the table, true symbols are used in $\varphi_t^*$ in the channel estimators. The right-hand columns show optimal adaptation gains $\mu$ and relative tracking noise levels (21) with prediction horizon $k = 4$ ($k = 3$ for LMS).

| | BER (%) | | | $\mu$ and V | | |
|---|---|---|---|---|---|---|
| SIR (dB): | 15 | 20 | 25 | 15 | 20 | 25 |
| DECISIONED REGRESSORS: | | | | | $\mu$: | |
| LMS | 8.3 | 4.1 | 1.9 | .31 | .31 | .36 |
| WLMS AR2 | 4.0 | .92 | .17 | .14 | .18 | .21 |
| WLMS AR2I | 4.0 | .85 | .12 | .13 | .15 | .17 |
| TRUE REGRESSORS: | | | | | V (dB): | |
| LMS | 2.8 | 1.1 | .62 | 5.8 | 9.0 | 13.1 |
| WLMS AR2 | 1.5 | .30 | .054 | 3.1 | 4.3 | 5.8 |
| WLMS AR2I | 1.5 | .28 | .044 | 2.9 | 3.7 | 4.8 |
| Known channel | 0.58 | .09 | .010 | 0 | 0 | 0 |

We use a recursively updated Viterbi detector [8, 11, 21] which needs to process its input over a few samples before a reliable symbol decision can be reached. A decision delay of three steps here provides the best performance. Due to an additional unavoidable delay in the regressor feedback loop, channel prediction $k = 4$ steps ahead is then required. For LMS, a decision delay of two steps provided the best performance.

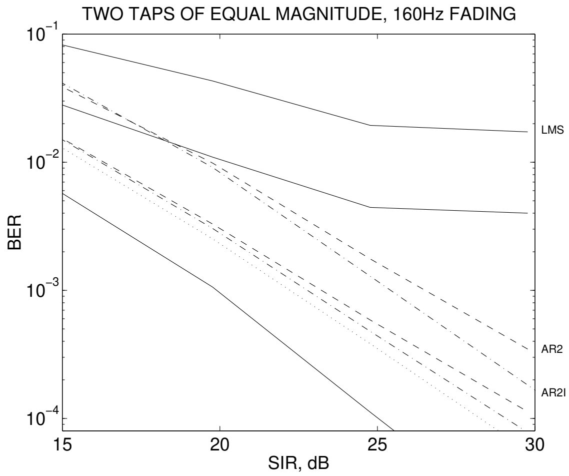


Figure 9: The Bit error rate as a function of the signal-to-interference ratio for the adaptive Viterbi equalizer. The BER with correct channel (lower solid) is compared to WLMS tracking with $AR_2I$ modelling with true $u_t$ as regressors (lower dash-dotted) and estimated regressors (upper dash-dotted) and to WLMS tracking with $AR_2$ modelling with true $u_t$ as regressors (lower dashed) and estimated regressors (upper dashed). Compare to LMS with optimized step length and true $u_t$ as regressors (middle solid) and with estimated regressors (upper solid). Also shown is $AR_2I$ tracking using true $u_t$ and correct initialization (dotted).

Figure 8 illustrates a rather typical tracking and bit error performance obtained at 20dB with $AR_2I$-based tracking. The estimates are initialized as linear trends. Everything goes well until the fading dip occurs at sample ~130, leading to several decision errors. When these errors are fed back as regressors to the tracker, they disturb the tracking in the interval 130-150. The system recovers after symbol no. 150.

More conclusions can be drawn from statistics on the BER when the correct $\Omega_D$ and signal-to-interference ratios (SIRs) are used in the design. Table 3, supported by Figure 9, presents the uncoded bit error rate for two-tap channels. Table 4 illustrates the flat fading case.

The performance indicator V from (21) in Table 3 and Table 4 provides adequate predictions of how much the BER plot for cases based on known regressors is shifted to the right, relative to the curve for a known channel.

Comparing the dotted to the lower dash-dotted curve in Figure 9 we see that not much performance is lost due to imperfect initialization. (If the algorithms were initialized with levels instead of linear trends, the performance would deteriorate further by 1-2dB.)

Decision-directed adaptation results in a performance loss due to nonlinear feedback effects caused by decision errors in the regressors. It is approximately 3dB for WLMS based on $AR_2$ and $AR_2I$ models in Figure 9.

In Table 3 and Figure 9, WLMS based on $AR_2I$ models show the best performance, but the performance of $AR_2$-based trackers is rather close. LMS tracking will in this case be completely inadequate, partly due to its inappropriate structure and not least due to its inability to predict the channels; With a random walk model, $\hat{h}_{t+k|t} = \hat{h}_{t|t}$. This results in a significant lag error, which will not vanish at low disturbance levels. Hence, the error floor at 1.7% BER. (Error floors also exist for the $AR_2$ and $AR_2I$-based designs, but they are far below the BER levels investigated in Figure 9.)

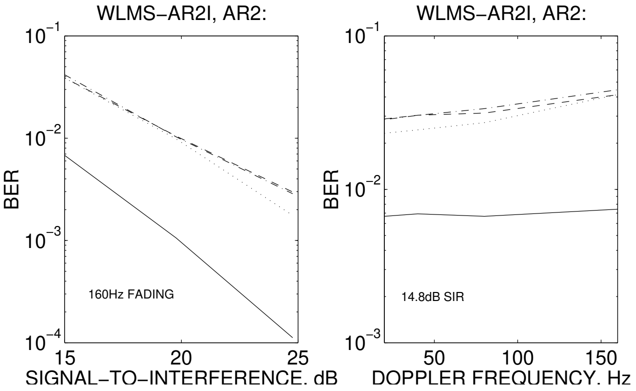


Figure 10: The BER as function of the SIR at 160Hz (left figure) and as a function of the Doppler frequency at 14.8dB SIR (right figure) for an adaptive Viterbi detector with k=4 step prediction. Performance of $AR_2I$-based (dash-dotted) and $AR_2$-based (dashed) WLMS channel estimators, *designed for SIR=15dB and* $f_D = 160Hz$. Compare to the performance of $AR_2$-based WLMS designed for the true SIR and $f_D$ (dotted) and to the performance for a known channel (solid).

To test our conclusions from Section VI.B, we have designed $AR_2$ and $AR_2I$-based WLMS algorithms for $f_D = 160$Hz and SIR=15dB and evaluated their performance at other operating points. The results, presented in Figure 10, confirm that one single fixed adaptive filter, designed at the high end of the uncertainty interval of the Doppler frequency and the low end of the SIR range can indeed be used over the whole parameter range. If the operating area is considered to be bounded by SIR=[15,25]dB and $f_D = [0, 160]$Hz, this filter does in fact constitute a minimax robust design, since the so-called saddle-point condition [9] is fulfilled: The resulting performance attains its worst value at the nominal (worst-case) design point. In the most critical regions, with low SIR and/or high Doppler frequency, the performance for an $AR_2I$-based design is about the same as for an $AR_2$-based design.

In the flat fading case, with $h_{1,t} = 0$, not much can be gained by improving the tracking. An exception is at high SNR, where for true regressors a significantly lower BER is attained for $AR_2$ or $AR_2I$-based designs than for LMS. This can be predicted by the values of V from (21) in the right-hand part of Table 4. For flat fading channels, all the algorithms provide about the same performance. The detector becomes trivially simple, so no channel prediction beyond $k = 1$ is required.

One can note an oddity in the results in Table 4: The BER is in several cases *lower* when a decisioned symbol is used as regressor, $\hat{y}_t = \hat{h}_t \bar{u}_t$, as compared to using

Table 4: Flat fading at $\Omega_D = 0.04$, $\mathrm{E}\,|h_{0,t}|^2 = 1, \mathrm{E}\,|h_{1,t}|^2 = 0$. 10000 slots are considered for each simulation case. In row 4 to 6, a true symbol is used as regressor. The relative noise level (V) is obtained with $k = 1$.

| | BER (%) | | | $\mu$ and V | |
|---|---|---|---|---|---|
| SNR (dB): | 15 | 20 | 25 | 15 | 25 |
| DECISIONED REGRESSORS: | | | | $\mu$: | |
| LMS | 2.8 | 1.00 | .36 | .39 | .73 |
| WLMS AR2 | 2.7 | 0.95 | .32 | .17 | .25 |
| WLMS AR2I | 2.7 | 0.96 | .33 | .14 | .19 |
| TRUE REGRESSORS: | | | | V (dB): | |
| LMS | 3.1 | 1.24 | .52 | 1.5 | 3.2 |
| WLMS AR2 | 3.2 | 1.12 | .37 | 0.7 | 1.2 |
| WLMS AR2I | 2.5 | 0.88 | .31 | 0.6 | 1.0 |
| Known channel | 2.1 | 0.69 | .23 | 0 | 0 |

the correct symbol $\hat{y}_t = \hat{h}_t u_t$. This effect is peculiar to *flat fading* channels on which *differential detection* and adaptive decision-directed receivers with *high gain* are used. As verified by simulation, a single error in a differential symbol normally results in two consecutive bit errors with correct channel estimates. In this case, the large estimation error $\varepsilon_t$ resulting from an incorrect regressor often causes the real part of $\hat{h}_{0,t}$ to start tracking the imaginary part of $h_{0,t}$ and $\mathrm{Im}(\hat{h}_{0,t})$ to track $\mathrm{Re}(h_{0,t})$, if the adaptation gain $\mu$ is high. This flip in the model tends to prevent the second bit error in the pair from occurring and thus to reduce the BER. The effect is strongest for LMS, which has the highest adaptation gain.

# VIII. Conclusions

In the IS-136 system, LMS adaptation is competitive only in the flat fading case. The WLMS algorithm provides efficient tracking also for two-tap channels. Our results indicate that a single tracking filter designed by underestimating the SIR and overestimating the Doppler speed could offer adequate performance over the entire range of operating conditions. Based on Figure 10, we conclude that the $\mathrm{AR}_2$ and $\mathrm{AR}_2\mathrm{I}$ designs provide equal performance in the worst cases, with high disturbance levels and/or fast fading. Due to its simple design, see Theorem 2 in [14], WLMS based on $\mathrm{AR}_2$ modelling becomes the preferred choice, as long as the parameters have zero mean.

The class of WLMS tracking algorithms provides a versatile tool for estimating fast fading channels. Their MSE performance can in the considered case be evaluated theoretically, which reduces the amount of simulation needed in the design of adaptive equalizers.

It should be noted, though, that the predicted steady-state MSE performance neglects initial transient effects. In practice, care must be taken in the initialization of the estimates, so that transient effects do not dominate the actual tracking performance over short data bursts.

It would be of value if tools could also be developed which model and predict the performance loss due to decision errors for adaptive receivers working in decision-directed mode. From simulations, our experience is that the gain $\mu$ that minimizes the bit error rate is somewhat higher than the gain that minimizes the MSE tracking performance for known regressors. Another possible generalization is to take information about the regressor uncertainty into account in the tracking design, as suggested in [16].

We have here evaluated the tracking algorithm without utilizing antenna diversity. High-performance channel trackers are, of course, of interest also in conjunction with multi-antenna receivers.

# References


[1] G. E. Bottomley and K. Molnar, "Adaptive channel estimation for multichannel MLSE receivers", *IEEE Communications Letters*, vol. 3, pp. 40-42, 1999.

[2] M-C. Chiu and C-C. Chao, "Analysis of LMS-adaptive MLSE equalization on multipath fading channels," *IEEE Trans. on Communications*, vol. 44, pp. 1684-1692, 1996.

[3] L. Davis, I. Collings and R. Evans, "Coupled estimators for equalization of fast-fading mobile channels," *IEEE Trans. on Comm.* vol. 46, pp. 1262-1265, 1998.

[4] T. Ekman, *Prediction of Mobile Radio Channels* Licentiate Thesis, Signals and Systems, Uppsala University, December 2000.

[5] N. C. Ericsson, S. Falahati, A. Ahlén and A. Svensson, "Hybrid type-II ARQ/AMS supported by channel predictive scheduling in a multi-user scenario," *IEEE Vehicular Technology Conference, Fall 2000* (VTC2000), Boston, MA, USA, September 24-28, 2000, pp 1804-1811.

[6] M. Falkenström, "A grid approach to tracking of mobile radio channels in D-AMPS 1900", Master Thesis, Report UPTEC 97 035E, Uppsala University, February 1997.

[7] W. C. Jakes, "Multipath Interference". In W. C. Jakes ed. *Microwave Mobile Communications.* Wiley, New York, NY, 1974. Reissued by IEEE, Piscataway NJ.

[8] K. Jamal, G. Brismark and B. Gudmundson, "Adaptive MLSE performance on the D-AMPS 1900 channel," *IEEE Trans. on Vehicular Technol.*, vol. 46, pp. 634-641, Aug. 1997.

[9] S. A. Kassam and V. Poor, "Robust techniques for signal processing: a survey," *Proc. of the IEEE*, vol. 73, pp. 433-481, 1985.

[10] L. Lindbom, "Simplified Kalman estimation of fading mobile radio channels: high performance at LMS computational load," *IEEE ICASSP* 1993, Minneapolis, MN, April 27-30, vol. 3 , pp. 352-355.

[11] L Lindbom, *A Wiener filtering approach to the design of tracking algorithms.* PhD Thesis, Dept. of Technology, Uppsala University, Sweden, 1995. www.signal.uu.se/Publications/abstracts/a951.html

[12] M. Sternad, L. Lindbom and A. Ahlén, "Tracking of time-varying systems, Part I: Wiener design of algorithms with time-invariant gains," Report, www.signal.uu.se/Publications/abstracts/r001.html

[13] A. Ahlén, L. Lindbom and M. Sternad, "Tracking of time-varying systems, Part II: Analysis of stability and performance of adaptive algorithms with time-invariant gains," Report, www.signal.uu.se/Publications/abstracts/r002.html

[14] L. Lindbom, M. Sternad and A. Ahlén, "Tracking of time-varying mobile radio channels. Part I: The Wiener LMS algorithm," *IEEE Transactions on Communications,* vol. 49, pp. xx-yy, 2001. www.signal.uu.se/Publications/abstracts/r003.html

[15] N. Lo, D. Falconer and A. Sheikh, "Adaptive equalization and diversity combining for mobile radio using interpolated channel estimates," *IEEE Trans. on Vehicular Technology*, vol. 40, pp. 636-645, 1991.

[16] A. Morgul and D. Dzung, "Decision directed channel parameter estimation and tracking using erroneous detectors," *Signal Processing*, vol. 25, pp. 307-318, 1991.

[17] J. Lin, J. G. Proakis, F. Ling and H. Lev-Ari, "Optimal channel tracking of time-varying channels: A frequency domain approach for known and new algorithms," *IEEE Trans. on Selected Areas in Commun.*, vol. 13, pp. 141-154, 1995.

[18] J. C. Martin and M. Mintz, "Robust filtering and prediction for linear systems with uncertain dynamics: a game-theoretic approach," *IEEE Trans. on Automatic Control.*, vol. 28, pp. 888-896, 1983.

[19] K. J. Molnar and G. E. Bottomley, "Adaptive array processing MLSE receivers for TDMA digital cellular PCS communications." *IEEE J. Selected Areas in Commun.*, vol. 16, pp. 1340-1351, 1998.

[20] "PCS IS136-based air-interface compatibility 1900MHz standard, Part I and II," SP 3388-1, SP 3388-2, J-STD-011.

[21] W. H. Sheen and G. L. Stüber, "MLSE equalization and decoding for multipath fading channels," *IEEE Trans. on Commun.*, vol. 39, pp. 1455-1464, 1991.

[22] M. Stojanovic, J.G. Proakis and J.A. Catipovic, "Analysis of the impact of channel estimation errors on the performance of a Decision-feedback equalizer in fading multipath channels," *IEEE Trans. on Communications*, vol. 43, pp. 877-886, 1995.

[23] M. Sternad and A. Ahlén, "Robust filtering and feedforward control based on probabilistic descriptions of model errors," *Automatica*, vol. 29, pp. 661-679, 1993.

[24] M. Sternad, L. Lindbom and A. Ahlén, "Robust Wiener design of adaptation laws with constant gains," *IFAC Workshop on Adaptation and Learning in Control and Signal Processing*, Como, Italy, August 2001.

[25] M.K. Tsatsanis, G.B. Giannakis and G. Zhou, "Estimation and equalization of fading channels with random coefficients," *Signal Processing*, vol. 53, pp. 211-229, 1996.

[26] K. Öhrn, A. Ahlén and M. Sternad, "A probabilistic approach to multivariable robust filtering and open-loop control." *IEEE Trans. on Automatic Control*, vol. 40, pp. 405-417, 1995.